

Effect of pH and annealing temperature on the structural and magnetic properties of cerium-substituted yttrium iron garnet powders produced by the sol-gel method

I. YARICI^{1*}, M. EROL², E. CELIK^{3,5}, Y. OZTURK^{1,4}

¹Department of Electrical and Electronics Engineering, Ege University, 35100, İzmir, Turkey

²Department of Materials Science and Engineering, Izmir Kâtip Celebi University, 35620, İzmir, Turkey

³Department of Metallurgical and Materials Engineering, Dokuz Eylul University, 35160, İzmir, Turkey

⁴Center for Production and Applications of Electronic Materials (EMUM), Dokuz Eylul University, 35160, Buca, Turkey

⁵Department of Nanoscience and Nanoengineering, Dokuz Eylul University, 35160, Buca, Turkey

Cerium substituted yttrium iron garnet ($\text{Ce}_{0.2}\text{Y}_{2.8}\text{Fe}_5\text{O}_{12}$; Ce-YIG) nanoparticles were produced via the sol-gel method from solutions of Ce-, Y- and Fe-based precursors, a solvent and a chelating agent. The solutions were dried at 200 °C and heat treated at temperatures between 800 °C and 1400 °C for 3 h in air. The effects of pH and annealing temperature on the structure, phase formation, magnetic properties and crystallite size were investigated. A cubic YIG phase was obtained for the sample annealed at 1400 °C. The presented results showed that the pH value of the starting solution affects the crystal size and consequently, the saturation magnetization.

Keywords: *sol-gel processes; Ce-YIG; nanoparticles*

© Wrocław University of Technology.

1. Introduction

Since the discovery of the yttrium iron garnet (YIG) structure, which has unique magnetic and magneto-optical properties, it has been the subject of extensive investigations [1, 2]. The results of these investigations have been used in several applications such as spatial light modulators, optical isolators, optical Faraday rotators, phase shifters, switches and sensors [1–8]. Nonetheless, the prospective applications of iron garnets require these materials to have superior magnetic and magneto-optical properties. As reported, the magnetic and magneto-optical properties of YIG are affected by the type and quantity of the substituted material, synthesis method and the microstructure of YIG particles [9–13]. Many studies have shown that the magneto-optical effects in iron garnets increase with the amount of substitution by

the elements such as Ce, La or Bi [14]. Compared with other substitutions, Ce is one of the most important ones, which has been found to increase the magneto-optical properties of an iron garnet [15].

The conventional method to synthesize YIG is the sintering of the corresponding oxides in a furnace at 1000 °C to 1400 °C, by a solid-state reaction [16]. However, this method uses different oxides and generally requires a pre-treatment to obtain the desired homogenous mixture [17]. In addition, an intermediate phase of YFeO_3 is also produced in a solid-state reaction, which is an undesirable phase for many applications. Alternatively, YIG structures can be synthesized by a variety of different wet chemical techniques, such as sol-gel, co-precipitation, micro-emulsion synthesis, citrate-gel routes, hydrothermal synthesis and glycothermal methods [18–32]. The sol-gel process can be given as an example of the most commonly used method. The sol-gel process offers

*E-mail: yariciismail@gmail.com

considerable advantages, including improved mixing of the starting materials and excellent chemical homogeneity in the final product. This method also does not require any expensive devices and vacuum, which is favorable for commercial production. Another important advantage is the easy control of the chemical composition of the target structure [27, 28]. For this method, the challenge is the influence of pH and chelation mechanism on the fabrication and crystallization of this compound [29]. In this manufacturing process, the Ce-YIG can be produced in the temperature range between 800 °C to 1400 °C [30, 31]. In literature, getting YIG phases via different methods have been reported [33, 34]. For example, by using the sol-gel method, Xu et al. [19] obtained a single phase of garnet structure at 850 °C, while Kum et al. [31] got a single phase garnet cubic structure only above 1200 °C [19, 31]. However, in another study using the proteic sol-gel method, the pure YIG phase could not be found even at 1100 °C [35]. Obtaining the intended phase at low temperatures is usually highly desirable for many applications, although this may turn into a disadvantage in high temperature fabrication processes. When the desired crystal structure is obtained at a low annealing temperature, using a higher annealing temperature causes the structure to decompose to intermediate phases such as α -Fe₂O₃ and YFeO₃ [27]. Our production method could be applied where the fabrication processes requires a high temperature treatment without the occurrence of secondary phases of YIG. This study can contribute to the high temperature chemical synthesis of pure and Ce-substituted YIG.

In the present study, Ce-YIG particles were synthesized using the sol-gel technique. The solvent to chelating agent ratio, as one of the important parameters of the sol-gel process, was examined. In addition, the structural and magnetic properties of the particles were investigated. The magnetic, structural and microstructural properties of the Ce-YIG powders were measured using X-ray diffraction (XRD), scanning electron microscopy (SEM) and a vibrating sample magnetometer (VSM). The measurements were interpreted with

the emphasis on coercivity and magnetization as a function of annealing temperature.

2. Experimental

Ce-substituted YIG particles (Ce-YIG) were prepared using an aqueous sol-gel method. The gel was obtained from aqueous solutions prepared from Ce-, Y- and Fe-based precursors, a solvent and a chelating agent. The precursor materials, Fe 2,4-pentanedionate (0.1774 mg), Y 2-ethylhexanoate (0.1458 mg) and Ce 2-ethylehexonate (0.014 mg), were dissolved in methanol and glacial acetic acid (GAA) in order to achieve a 0.23 M solution with the chemical composition Ce:Y:Fe = 0.2:2.8:5. Ce-YIG powders were produced from the starting solutions of different pH values. The pH values for 3.5 mL solutions containing 3 mL, 2 mL, 1.5 mL and 1 mL GAA were found to be 1.1, 2.05, 2.45 and 2.9, respectively. A higher GAA concentration led to lower pH values, and lower GAA concentration led to poorly dissolved precursors. The prepared solutions were dried at 200 °C and annealing treatments were performed at temperatures ranging from 800 °C to 1400 °C for 3 h in air.

XRD studies were performed on a Shimadzu X-ray diffractometer operating with CuK α radiation ($\lambda = 0.15405$ nm). The morphology and the particle sizes of the samples were observed using a Phillips XL-30S field emission gun SEM. Magnetic measurements were carried out at room temperature using a VSM (Digital Measurement System JDM-13) by applying the maximum magnetic field of 3500 Oe.

3. Results and discussion

The solution with the pH value of 2.45 was chosen to investigate the effect of annealing temperature. Fig. 1 shows the XRD patterns of the Ce-YIG powders that were annealed at different temperatures from 800 °C to 1400 °C for 3 h in air. The cubic garnet structure of YIG started to form at annealing temperatures higher than 900 °C. The samples annealed below 1000 °C showed mixed phases of YFeO₃, CeO₂, α -Fe₂O₃, Y₂O₃

and garnet structures. As the annealing temperature increased, the reaction between mixed phases accelerated. This reaction led to the formation of the cubic garnet phase and secondary phases such as YFeO_3 and perovskite garnet. The powders annealed above $1000\text{ }^\circ\text{C}$ showed the garnet cubic structure as a dominant phase. Furthermore, most of the mixed and secondary phases were no longer present when the samples were annealed at $1400\text{ }^\circ\text{C}$. From the XRD results, the garnet formation can be summarized by indicating that the whole process includes four steps: the removal of solvent based materials, combustion of carbon-based content, formation of oxides and garnet formation.

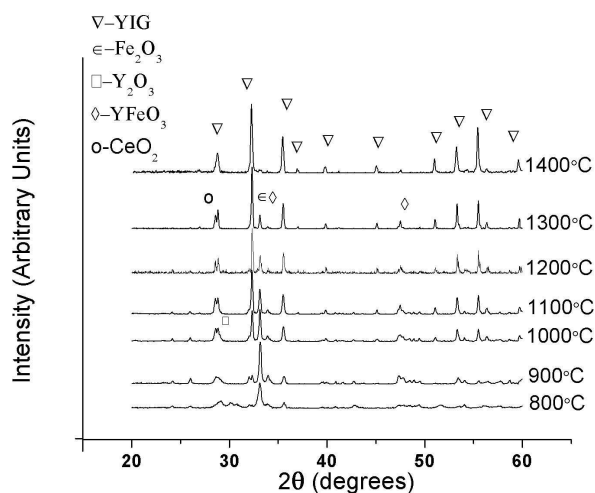


Fig. 1. X-ray diffraction patterns of the garnet powders produced with a precursor solution at pH 2.45 and annealed at temperatures from $800\text{ }^\circ\text{C}$ to $1400\text{ }^\circ\text{C}$.

Thin film samples prepared from the same solutions were based on completely different crystallization dynamics. Single phase thin films of iron garnet coated on Si (1 1 1) and fused silica were obtained at annealing temperatures of $900\text{ }^\circ\text{C}$ and $800\text{ }^\circ\text{C}$, respectively [27]. Our previous results indicated that the substrate solution interactions lowered the crystallization temperature of the thin films [27].

Fig. 2 shows the results for YIG precursor annealed at pH values of 1.1, 2.05, 2.45 and 2.9. Secondary phases started to appear for

the sample prepared from a solution with pH of 2.9. Several studies have shown that increasing the pH value of the solution has a negative effect on the garnet phase [29, 32]. However, in our samples the main reason for the appearance of secondary phases might be the decrease of precursor solubility. Samples with lower pH values indicate that the obtained powder has a single phase iron garnet structure.

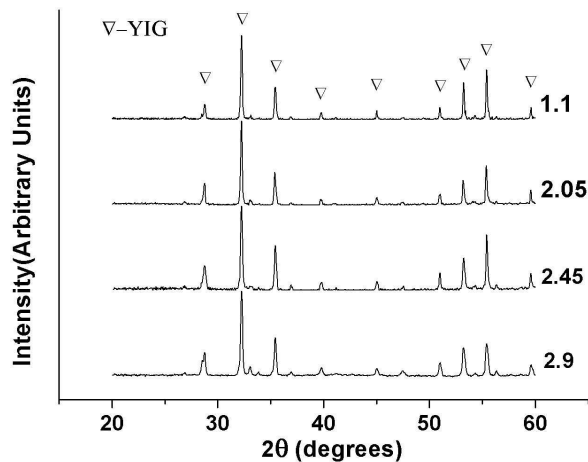


Fig. 2. X-ray diffraction patterns of the garnet powders annealed at $1400\text{ }^\circ\text{C}$ obtained from solutions of pH values between 1.1 and 2.9.

The SEM studies of the garnet powders heat treated at different temperatures revealed their phase and morphological structures. Fig. 3 shows SEM images of the samples heat treated at $800\text{ }^\circ\text{C}$, $1100\text{ }^\circ\text{C}$ and $1400\text{ }^\circ\text{C}$ for 3 h in air. The results show that the particles have irregular shapes, and are nano- and micro-sized. Increasing the annealing temperature causes an increase in both crystallite and grain size, and the grains are fused and necked to each other, forming agglomerated structures. The particles become rounder and larger with smoother surfaces as the annealing temperature increases. The samples annealed at $800\text{ }^\circ\text{C}$ (Fig. 3a) show a porous structure. As the annealing temperature increases, the porous structure converts to a fine-grained structure, and traces of melted regions are present as shown in Fig. 3b. The size of the roughly spherical shapes of the samples prepared at $1400\text{ }^\circ\text{C}$ is smaller than that of the samples prepared by the proteic sol-gel process method, but

larger than of the samples prepared by the auto-combustion of nitrate-citrate gel and sonochemical synthesis methods [34, 35].

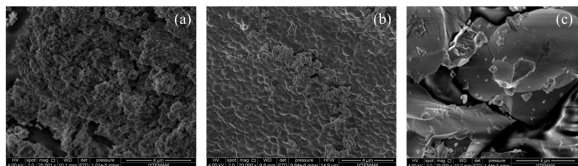
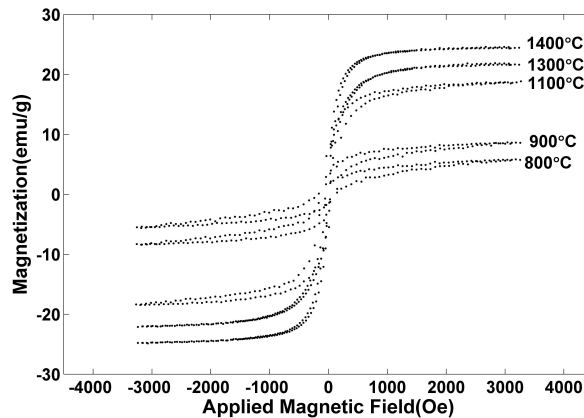


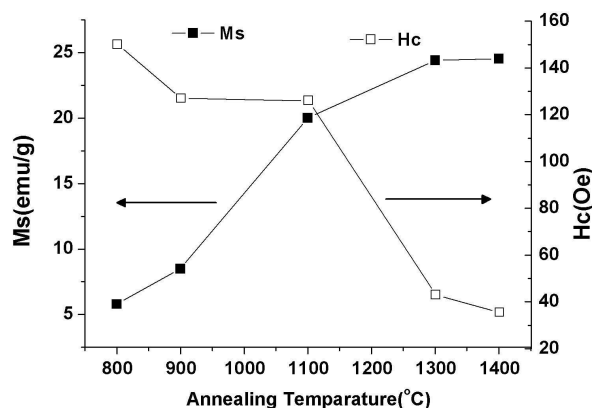
Fig. 3. SEM images of the garnet samples heat treated at (a) 800 °C, (b) 1100 °C and (c) 1400 °C.

In order to clarify the correlation between the coercivities and saturation magnetization and the annealing temperatures, we measured hysteresis of the powders using VSM (Fig. 4a). Fig. 4b shows the coercivities and the saturation magnetization for different annealing temperatures of the Ce-YIG powders. The magnetization value increases with increasing annealing temperature; however, the coercivity decreases which is consistent with the other studies on solid state reaction, auto combustion process and plasma spraying technique [9, 17]. The saturation magnetization of the garnet powder annealed at 1400 °C was $M_s = 24.5$ emu/g. One feature of garnet powders is that the crystallite size influences the magnetic properties. To evaluate the magnetic properties of the garnet powders as a function of crystallite size, their sizes were calculated using the XRD results. The crystallite sizes ranged from 38 nm to 55 nm. The crystallite sizes increased as the annealing temperature increased from 800 °C to 1400 °C because of increased nucleation, and the crystallization of the samples was completed as shown in Fig. 1. Moreover, the powders annealed at 1400 °C had the lowest coercivity value $H_c = 35.5$ Oe among all the samples.

Compared with the garnets prepared by other methods, such as auto-combustion process and precursor plasma spraying technique, whose saturation magnetization values reported in the literature were 25.85 emu/g and 23.7 emu/g, respectively, the saturation magnetization of our garnet (24.5 emu/g) is close to the commonly observed results and the reported YIG bulk value (26 emu/g). In addition, the presented coercivity changes



(a)



(b)

Fig. 4. VSM results of samples annealed between 800 and 1400 °C: (a) hysteresis curves and (b) coercivity and saturation magnetization values against annealing temperature.

of YIG garnets are similar to the results of other common methods where the coercivity decreases with the increasing annealing temperatures as discussed previously [9, 17].

The results will be discussed considering the effects of Ce substitution, particle size, crystallization and impurity phases. YIG has a complex cubic structure, wherein nonmagnetic Y^{3+} ions occupy dodecahedral (c) sites and magnetic Fe^{3+} ions occupy octahedral (a) and tetrahedral (d) sites. The unit cell includes different magnetic ions, iron and one element of the rare earth group. The magnetic properties arise from the antiparallel ordering between Fe^{3+} ions in the a- and d-sites as a result of exchange couplings between the ions, but

the c-site ions couple weakly, leading to their displacement anti-parallel to the d-site ion [36, 37]. The net magnetic moment of a YIG per unit cell is 40 Bohr magnetons [38]. With the addition of Ce, paramagnetic trivalent Ce^{3+} ions are replaced with nonmagnetic Y^{3+} ions in c-sites [39], which is expected to slightly increase the saturation magnetization because of the paramagnetic Ce ions. There are several studies about the particle size magnetization relationship, reporting that an increase in particle size (45 nm to 450 nm) causes an increase in magnetization [40, 41]. In conclusion, the increased particle size has a positive effect on saturation magnetization. The tendency of M_s to increase is consistent with the enhancement of crystallinity. With an increasing annealing temperature, the amounts of both antiferromagnetic $YFeO_3$ and weak ferromagnetic $\alpha-Fe_2O_3$ parasitic phases decrease. The coercivities of these structures are higher than that of YIG [42]. The coercivity of magnetic materials depends on their production method, size, impurities and shape. Therefore, the decrease in the non-magnetic impurities and magnetic parasitic phases in the structure leads to a decrease in coercivity of samples annealed at higher temperatures. These results are in accordance with the XRD and SEM analyzes.

Magnetization, crystallite size and pH results of the samples are presented in Fig. 5 in order to explain the relationships between these parameters. The crystallite sizes of the samples were estimated from the line width of the (4 2 2) XRD peaks, and calculated using Scherrer's relationship $D = k\lambda/B \cos\theta$, where 'D' is the average diameter in nm, 'k' is the shape factor, 'B' is the broadening of the diffraction line measured at half of its maximum intensity in 'radians', ' λ ' is the wave length of X-ray and ' θ ' is the Bragg's diffraction angle. As the crystallite size increases, saturation magnetization increases. Vajargah *et al.* [32] studied the relationship between the crystallite size of particles and pH values. Our study supports their findings about the relationship between magnetic properties and crystallite size of YIG powders, although their synthesis mechanism was sol-gel combustion method. The relationship between pH and crystallite size is

not linear, which may be caused by the effect of pH on the oxidation process of Fe, Ce and Y during the heat treatment [43]. As shown in Fig. 5, the pH of the initial solution was important to the magnetization dynamics and crystallite size. The crystallite size reaches a maximum of 51 nm for the sample with a pH value of 2.45. The maximum saturation magnetization value was measured as 25.2 emu/g for the sample with the maximum crystallite size. This value is slightly lower than that of the bulk YIG (26 emu/g).

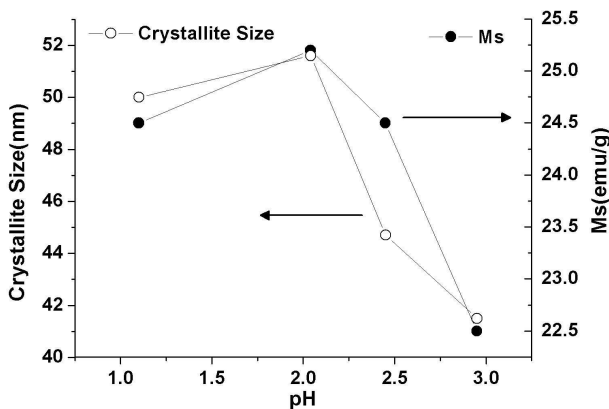


Fig. 5. Crystallite size and magnetization at different pH values of initial solutions annealed at 1400 °C.

4. Conclusions

$Ce_{0.2}Y_{2.8}Fe_5O_{12}$ garnets were prepared using sol-gel method. XRD patterns indicated that powder annealing at low temperatures produced mixed phases. However, the sample annealed at 1400 °C contained the cubic garnet phase. SEM images showed that increasing the annealing temperature caused an increase in grain size, and the grains were fused and necked to each other, forming an agglomerated structure. Magnetic M-H loops were observed, and the coercivity and saturation magnetization of Ce-YIG powder annealed at 1400 °C was $H_c = 35.5$ Oe and $M_s = 24.5$ emu/g, respectively. The saturation magnetization increased with increasing annealing temperatures whereas the coercivity values decreased. The pH value affected crystal size and as a result, the saturation magnetization value. Secondary phases started to appear

for the samples prepared with solutions of high pH values. The maximum saturation magnetization value of 25.2 emu/g was obtained for the sample annealed at 1400 °C at a pH value of 2.45, showing the maximum crystallite size of 51 nm.

References

- [1] GELLER S., GILLES M.A., *Acta Crystallogr.*, 10 (1957), 239.
- [2] HUANG B., REN R., ZHANG Z., ZHENG S., *J. Alloy. Compd.*, 558 (2013), 56.
- [3] PRIYE V., BISHNU P.P., THYAGARAJAN K., *J. Light-wave Technol.*, 16 (2) (1998), 246.
- [4] SEKIJIMA T., FUJII T., WAKINO K., OKADA M., *IEEE T. Microw. Theory*, 47 (12) (1999), 2294.
- [5] GOLDMAN A., *Technological Ferrites*, Oxford Publications, 1990.
- [6] STANDLEY K.J., *Oxide Magnetic Materials*, 2. Edn. Clarendon Press, Oxford, 1972.
- [7] YAHYA N., HEAN G.K., *Am. J. Applied Sci.*, 4 (2) (2007), 80.
- [8] LEE J.W., OH J.H., LEE J.C., CHOI S.C., *J. Magn. Magn. Mater.*, 272 (2004), 2230
- [9] GUO X.Z., RAVI B.G., DEVI P.S., HANSON J.C., MARGOLIES J., GAMBINO R.J., PARISE J.B., SAMPATH S., *J. Magn. Magn. Mater.*, 295 (2005), 145.
- [10] VAQUEIRO P., CROSNIER-LOPEZ M.P., LOPEZ-QUINTELA M.A., *J. Solid State Chem.*, 126 (1996), 161.
- [11] INOUE M., NISHIKAWA T., NAKAMURA T., INUI T., *J. Am. Ceram. Soc.*, 80 (8) (1997), 2157.
- [12] KURODA C.S., TANIYAMA T., KITAMOTO Y., YAMAZAKI Y., *J. Magn. Magn. Mater.*, 241 (2002), 201.
- [13] MATSUMOTO K., YAMAMOTO S., YAMANOE Y., UENO A., YAMAGUCHI K., FUJII T., *Jpn. J. Appl. Phys.*, 30 (1991), 1696.
- [14] KIM T., NASU S., SHIMA M., *J. Nanopart. Res.*, 9 (2007), 737.
- [15] GOMI M., FURUYAMA H., ABE M., *J. Appl. Phys.*, 70 (11) (1991), 7065.
- [16] NIYAFAR R.M., RADHAKRISHNA M.C., HASSNPOUR A., MOZAFFARI M., AMIGHIAN J., *Hyp. Interact.*, 187 (2008), 137.
- [17] MAO T.C., CHEN J.C., *J. Magn. Magn. Mater.*, 302 (1) (2006), 74.
- [18] KUM J.S., KIM S.J., SHIM I.B., KIM C.S., *IEEE T. Magn.*, 39 (5) (2003), 3118.
- [19] XU H., YANG H., *J. Mater. Sci.-Mater. El.*, 19 (2008), 589.
- [20] GARSKAITE E., GIBSON K., LELECKAITE A., GLASER J., NIZNANSKY D., KAREIVA A., MEYER H.J., *Chem. Phys.*, 323 (2006), 204.
- [21] CHENG Z., YANG H., YU L., XU W., *J. Mater. Sci.-Mater. El.*, 19 (2008), 442.
- [22] NGUYET D.T.T., DUONG N.P., SATOH T., ANH L.N., HIEN T.D., *J. Alloy. Compd.*, 541 (2012), 18.
- [23] RASHAD M.M., HESSIEN M.M., EL-MIDANY A., IBRAHIM I.A., *J. Magn. Magn. Mater.*, 321 (2009), 3752.
- [24] WEI Z., CUIJING G., RONGJIN J., CAIXIANG F., YANWEI Z., *Mater. Chem. Phys.*, 125 (2011), 646.
- [25] VAQUEIRO P., LOPEZ-QUINTELA M.A., RIVAS J., GRENECHE J.M., *J. Magn. Magn. Mater.*, 169 (1997), 56.
- [26] CHO Y.S., BURDICK V.L., AMARAKOON V.R.W., *J. Am. Ceram. Soc.*, 80 (6) (1997), 1605.
- [27] OZTURK Y., EROL M., CELIK E., MERMER O., KAHRAMAN G., AVGIN I., *Mater. Tehnol.*, 47 (1) (2013), 59.
- [28] REHSRINGER J.L., BURSİK J., NIZNANSKY D., KLARIKOVA A., *J. Magn. Magn. Mater.*, 211 (2000), 291.
- [29] VAJARGAH S.H., HOSSEINI H.R.M., NEMATİ Z.A., *Mater. Sci. Eng. B-Adv.*, 129 (2006), 211.
- [30] XU H., YANG H., XU W., FENG S., *J. Mater. Process. Tech.*, 197 (2008), 296.
- [31] KUM J.S., KIM S.J., SHIM I., KIM C.S., *J. Magn. Magn. Mat.*, 272 (2004), 2227.
- [32] VAJARGAH S.H., HOSSEINI H.R.M., NEMATİ Z.A., *J. Alloy. Compd.*, 430 (2007), 339.
- [33] JESUS F.S., CORTES C.A., VALENZUELA R., AMMAR S., BOLARIN-MIRO A.M., *Ceram. Int.*, 38 (2012), 5257.
- [34] PINKAS J., REICHOVA V., SERAFIMIDISOVA A., MORAVEC Z., ZBORIL R., JANCİK D., BEZDICKA P., *J. Phys. Chem. C*, 114 (32) (2010), 13557.
- [35] LABUAYAI S., SIRI S., MAENSIRI S., *J. Optoelectron. Adv. M.*, 10 (2008), 2694.
- [36] SEKIJIMA T., KISHIMOTO H., FUJII T., WAKINO K., OKADA M., *Jpn. J. Appl. Phys.*, 38 (1999), 5874.
- [37] HENCH L.L., WEST J.K., *Principles of Electronic Ceramics*, Wiley, New York, 1990.
- [38] MOULSON A.J., HERBERT J.M., *Electroceramics: Materials, Properties, Applications*, Wiley, West Sussex, 2003.
- [39] WICKERSHEIM K.A., BUCHANAN R.A., *J. Appl. Phys.*, 38 (1967), 1048.
- [40] XU H., YANG H., *Mat. Manuf. Process.*, 23 (1) (2007), 1.
- [41] SANCHEZ R.D., RIVAS J., VAQUEIRO P., LOPEZ-QUINTELA M.A., CAEIRO D., *J. Magn. Magn. Mat.*, 247 (2002), 92.
- [42] MITRA S., DAS S., MANDAL K., CHAUDHURI S., *Nanotechnology*, 18 (2007), 275608.
- [43] PRAVEENA K., SADHANA K., SRINATH S., MURTHY S.R., *Mater. Res. Innov.*, (2013), 1.

Received 2015-09-27

Accepted 2016-01-18